



Contents lists available at ScienceDirect

Arabian Journal of Chemistry

journal homepage: www.ksu.edu.sa

Original article

Photo-enhanced catalytic activity enabled by core-shell nanozymes for combination breast cancer therapy

Xue Meng, Juan Gao*

Department of Radiation Oncology, Affiliated Cancer Hospital of Inner Mongolia Medical University & Peking University Cancer Hospital of Inner Mongolia Campus, No. 42 Zhaowuda Road, Saihan District, Hohhot 010020, China

ARTICLE INFO

Keywords:

Breast cancer
Core-shell
Nanozymes
Photodynamic
Chemotherapy

ABSTRACT

Enhanced catalytic therapy of triple-negative 4T1 breast tumors through the application of photo-enhanced peroxidase (POD)-like and catalase (CAT)-like activities combined with chemotherapy could be enabled by core-shell nanozymes. Therefore, the dual POD and CAT-like activities of the core-shell iron oxide (Fe₃O₄)-@gold (IO@Au) nanozymes loaded with epirubicin (EPI) were evaluated in this study for photo-enhanced combination therapy. The core-shell nanozymes induced oxidative stress and apoptosis, and these effects were enhanced upon application of PDT, as demonstrated by ROS and caspase-3 activity assays. Additionally, it was shown that by reducing the expression of HIF-1 α gene and upregulation of caspase-3 gene, core-shell nanozymes with and without PDT were able to induce a significant reduction in tumor weight, when compared to free EPI. The bio-distribution of the drug-loaded into core-shell nanozymes showed a higher accumulation of the EPI in the 4T1 breast tumor when compared to samples treated with free EPI. Overall core-shell nanozymes with catalytic-like activity can be used as potential platforms for photo-enhanced combination therapy.

1. Introduction

Chemotherapy, one of the most employed approaches in the treatment of cancer, has significantly improved over the recent years. However, remarkable adverse effects due to the limited targeting potency and upregulation of chemo-resistance signaling pathways reduce the efficacy of chemotherapy. Consequently, some cancer types, especially chemo-resistant ones, only benefit from modest treatment outcomes (Lee et al., 2018). Therefore, the application of therapeutic systems enabling the development of combination therapy, employing two or more medications with a single platform, has been recommended (Sharifi et al., 2020, Khan et al., 2023). Therefore, a combination of chemotherapy and other therapeutic approaches has been extensively applied to the treatment of a wide range of cancers in order to manage the adverse effects against off-target tissues and facilitate the chemotherapeutic potency (Lane, 2006, Mokhtari et al., 2017). When combined with chemotherapy, photodynamic therapy (PDT), which kills tumor cells by utilizing a singlet oxygen molecule, can further restrict the growth of cancer cells than a single modality approach, making it more effective at combating cancer cells and even overcoming hypoxia.

Nanomedicine can play a key role in the development of combination therapeutic systems. In fact, nanomaterials-mediated cancer therapy plays a crucial role in promoting therapeutic efficacy against cancer through recruiting a combination of nano-based platforms and chemotherapeutics. Therefore, combination therapy has been demonstrated to facilitate the control of tumor growth while reducing unwanted side effects through regulating the pharmacokinetics and targeted drug distribution (Gurunathan et al., 2018).

For example, Lee et al., (Lee et al., 2018) and Li et al., (Li et al., 2016) by combination of chemotherapy with PDT enabled by developed nanoplateforms, were able to inhibit the proliferation of pancreas and breast malignancies mediated by boosting single oxygen in tumor tissues. However, their findings suggest that the oxygen supply in malignant tissues is insufficient to generate a significant amount of single oxygen.

Core-shell nanostructures, different materials for the core and the shell, have shown significant benefits over classical counterparts causing the improvement of some unique characteristics such as (i) more biocompatibility and catalytic-like activities, (ii) less aggregation tendency, (iii) feasible functionalization with other biomolecules, and (iv)

* Corresponding author at: Department of Radiation Oncology, Affiliated Cancer Hospital of Inner Mongolia Medical University & Peking University Cancer Hospital of Inner Mongolia Campus, Hohhot 010020, China.

E-mail address: Miyuki1207@126.com (J. Gao).

<https://doi.org/10.1016/j.arabjc.2024.105626>

Received 29 November 2023; Accepted 9 January 2024

Available online 11 January 2024

1878-5352/© 2024 The Authors. Published by Elsevier B.V. on behalf of King Saud University. This is an open access article under the CC BY-NC-ND license (<http://creativecommons.org/licenses/by-nc-nd/4.0/>).

higher stability (Chatterjee et al., 2014, Khan et al., 2023, Li et al., 2023). Therefore, core-shell nanostructures have been shown to serve as effective photosensitizers for potential PDT against cancer through controllable singlet-oxygen formation provided with their catalytic-mimic functions. In fact, the successful elimination of tumors *in vivo* provided additional evidence of the excellent therapeutic impacts of core-shell biocatalysts (Khan et al., 2023).

Although the combination of PDT with iron oxide (IO)-based nanozymes showing POD-mimic activity can increase the generation of reactive oxygen species (ROS) for cancer therapeutics (Gao et al., 2017a), it seems that the usage of other nanomaterials such as platinum (Pt), gold (Au), or silver as shell modifier (Xu et al., 2022, Sharifi et al., 2023) can increase the combinatory cancer therapeutics through POD-mimic activity and CAT-mimic activity. In this line, it was shown that the application of Au/IO hybrid nanoparticles significantly improves breast cancer therapeutics enabled by their enzyme-mimic activity (Zeng et al., 2023). Also, it has been revealed that the Au-anchored Fe single-atom nanozymes can be used for biocatalysis and enhanced tumor therapy (Feng et al., 2022). The penetration of the drug into the tumor tissue and Photo-enhanced accumulation of ROS and singlet oxygen in the tumor microenvironment enabled by core-shell nanozymes promise to significantly improve cancer combination therapy.

Therefore, to modulate the treatment of breast cancer, as a tumor model used in this study, based on a combination of chemotherapy and PDT, we used core-shell IO@Au nanozymes loaded with epinephrine (EPI) as a potential therapeutic platform. In fact, triple-negative (ER-negative, PR-negative, HER2/neu not overexpressed) breast cancer has shown well-defined clinical and pathologic characteristics, and due to its comparatively poor prognosis, aggressive nature, and no defined targeted modalities, which leaves chemotherapy as the basis of treatment, this malignancy is regarded as clinically concerning (Irvin and Carey, 2008).

The ability of core-shell nanozymes to mimic the CAT-like activity allowed for PDT to be achieved. Additionally, the POD-like activity of core-shell nanozymes loaded with EPI led to a significant production of ROS, which can induce apoptosis. Also, core-shell nanozymes loaded with EPI allowed for the pH-sensitive drug release to enhance smart drug delivery. Increasing the lifespan of EPI in the blood while reducing its accumulation in off-targeted tissues, decreasing the growth of breast cancer cells, and overcoming the hypoxia level of malignant tissues all appear to be tremendous achievements in the treatment of breast cancer enabled by core-shell nanozymes.

2. Experimental section

2.1. Materials

Spherical iron oxide gold nanozymes (IO@Au, 99 %, core (Fe₃O₄): 80–100 nm, shell (Au): 20–30 nm) were purchased from Nanoshell Co. (Wilmington DE, USA, <https://www.nanoshel.com/product/iron-oxide-gold-core-shell-nano-particles>).

Epirubicin hydrochloride (≥ 90 %, HPLC) and 3-(4,5-dimethylthiazol-2-yl)-2,5-diphenyl-2H-tetrazolium bromide (MTT) were purchased from Sigma-Aldrich (St. Louis, USA). Dulbecco's modified Eagle's medium (DMEM), streptomycin and Fetal Bovine Serum (FBS) were purchased from Gibco (Germany). Mouse breast carcinoma 4T1 cells were received from Shanghai Cell Bank of the Chinese Academy of Sciences (Shanghai, China). All other materials were from Merck Co. (Darmstadt, Germany).

2.2. Preparation of IO@Au nanozymes loaded with EPI

20 mL of core-shell nanozymes (5 mg/mL) was sonicated with 5 mL stock solution of EPI (5 mg/mL) for 50 min and then stirred gently overnight at room temperature. Afterward, the nanozymes separated using an external magnet device were washed with dry ethanol three

times. The EPI concentration in the solution was analyzed using a standard drug concentration curve obtained with a UV-Visible spectrophotometer at 500 nm.

2.3. Determination of drug loading (DL) and encapsulation efficacy (EE)

To quantify the loading efficiency of the EPI in the core-shell IO@Au nanozymes, DL% and EE% were evaluated as described previously by Darnafar et al (Danafar et al., 2018).

2.4. Drug release study

EPI release from IO@Au nanozymes was obtained during 12 h at pH 7.4 and 6.5. Nanozymes (20 mg) dissolved in 10 mL of phosphate-buffered saline (PBS) buffer into the dialysis bags at 37 °C were exposed to gentle shaking. 1 mL of samples were removed and replaced with 1 mL of the same fresh PBS buffer. Drug releases were evaluated within different time intervals by a UV-visible spectrophotometer at 500 nm.

2.5. Enzyme-like activity assay

Peroxidase (POD)-like activity of core-shell nanozyme was determined through the oxidation of the 3,3',5,5'-tetramethylbenzidine (TMB) in TMB-H₂O₂ solution at pH 4 based on the method reported previously (Lu et al., 2016). After the reaction, the solutions were examined by UV-vis spectroscopy (Shimadzu UV-2600).

Catalase (CAT)-like activity of core-shell nanozymes was done based on the method reported previously (Alizadeh et al., 2021). The photo-enhanced enzyme-like activity was carried out by exposure to irradiation with a 30 mW/cm² laser and a final dose 6.4 J/cm² at various time points during the treatment.

2.6. Cell culture

The mice breast cancer cell line, 4T1, was cultured in DMEM and 10 % FBS along with 1% antibiotics at 5 % CO₂ at 37 °C.

2.7. MTT assay

The cytotoxic effects of free EPI (10 µg/ml), as well as IO@Au nanozyme loaded with EPI (equivalent concentration to 10 µg/ml EPI) in the absence and presence of PDT on 4T1 cell line, were evaluated by the MTT assay. Briefly, cells plated at a density of 1×10^4 cells per well for 24 h were then exposed to a series of samples for an additional 24 h. To evaluate the effect of PDT, after 8 h, samples were irradiated with a laser having a power intensity of 30 mW/cm², an irradiation time of 5 min, and a final dose of 6.4 J/cm². Then, 20 µL MTT solution was added to each well and incubated for 3 h at 37 °C in the dark. After gentle removal of medium, 150 µL DMSO was added per well and incubated for an additional 15 min. The absorbance of the samples was detected at 570 nm using a microplate reader (Tecan Spark 10 M, Tecan, Switzerland).

2.8. Caspase-3 assay

To evaluate the induction of apoptosis, 1×10^5 cells were seeded in six-well plates and incubated at 37 °C with 5 % CO₂ overnight. Subsequently, free EPI (10 µg/ml) as well as IO@Au nanozymes loaded with EPI (equivalent concentration to 10 µg/ml EPI), were added to the 4T1 cell culture medium and incubated for 24 h. After 8 h, the samples were irradiated with a 30 mW/cm² laser for 5 min (the final dose of 6.4 J/cm²). Then, the cells were collected, centrifuged at 1000g (5 min), washed in cold PBS, and lysed with cell lysis buffer provided with the Kit (Cell Signaling Technology, USA) for 30 min on ice. Afterward, samples were centrifuged at 15,000 × g for 10 min at 4 °C and the protein

concentrations in supernatants were determined by Bradford protein assay kit (Sigma, USA). Then, 100 µg protein from each sample was used for caspase-3 activity assay based on the protocols provided by the Caspase-3 Assay Kit (Colorimetric) (ab39401). The absorbance was recorded at 405 nm using a microplate reader (Tecan Spark 10 M, Tecan, Switzerland).

2.9. ROS assay

2,7-DCF-diacetate (DCFH-DA), a non-fluorescent permeable probe, was used to assess the ROS level in cancer cells. Accordingly, after treating the cells as described in section 2-8, the samples were added by 30 µM DCFH-DA for 30 min. Afterwards, the fluorescence intensity was recorded at Ex/Em = 485/535 nm by fluorometric microplate reader.

2.10. In-vivo trials

2.10.1. Animal and tumor model

To investigate the effects of the drug and nanozymes on cancer therapeutics, female BALB/C mice (6-old week) weighing approximately 23 g were used and treated based on ethical guidelines. Subsequently, 6×10^5 cultured 4T1 cancer cells were injected and monitored through subcutaneous injection at the end of the left mammary gland. When the tumor size reached about $\sim 200 \text{ mm}^3$ after 25 days, 32 mice were divided into 4 groups including control, EPI (10 mg/kg), and core-shell nanozymes loaded with EPI (with or without PDT) and the EPI and nanocarriers were administrated through tail injection on days of 1, 6, 12, 18, 24, and 30.

2.10.2. PDT, weight of mice and tumor volume

For PDT performance, all tumors were treated percutaneously with irradiation at 420 mW/cm² laser for 5 min at a final dose of 100 J/cm² every 3 days and 8 h after injection of nanozymes, through the surface of the skin with a 10 mm spot diameter.

The weight of mice and tumor volume were measured and recorded every 6 days. A digital vernier caliper was used to determine the tumor volume and calculate the amount of changes in tumor volume during the study time based on the equation $V(\text{mm}^3) = (D \times d^2)/2$ (D is long diameter and d is short diameter). The rate of change in the tumor volume was then recorded. At the end of the trial, the mice were sacrificed and tumors were collected and weighed.

2.10.3. Quantitative real-time PCR (qRT-PCR)

Tumor tissues from various treated groups was quickly frozen in nitrogen fluid and the total RNA was extracted using the TRI reagent (Invitrogen) in accordance with the manufacturer's instructions. The acquired RNA's purity and concentration were assessed using a Nanodrop spectrophotometer (Thermo Fisher Scientific). The revert Aid First Strand cDNA Synthesis Kit (Fermentas) was then used to create single-stranded complementary DNA (cDNA). Following that, qRT-PCR was used to amplify the generated samples using SYBR Premix Ex Taq II (Tli RNaseH Plus). According to the protocol, the thermal cycle used consists of a primary phase at 95 °C for 2 min, a denaturation phase at 95 °C for 10 s, 39 cycles for annealing/expansion at 60 °C for 30 s and 65–95 °C for 5 s on the melting curve. PCR primers used were as follows: β-actin (243 bp):

F-5'-CTTCTACAATGAGCTGCGTG-3', R-5'-TCATGAGGTAGTCAGTCA GG-3';

caspase-3 (400 bp):

F-5'-TTTGTGTTGTGTGCTTCTGAGCC-3', R-5'-ATTCTGTTGCCACCTTT CGG-3';

HIF-1α (151 bp):

F-5'-AGCTTCTGTTATGAGGCTCACC-3'; R-5'-TGACTTGATGTTTCATC GTCTC-3'

The expression of target RNA relative to the housekeeping gene was calculated based on the threshold cycle (Ct) as $R = 2^{-\Delta(\Delta C_t)}$.

2.10.4. Iron and drug distribution

In order to evaluate the distribution of Fe in vital tissues, including the liver, kidney, spleen, brain and tumor, at the end of the experiment (30th day), the tissues were digested in a mixture of hydrochloric acid and nitric acid (ratio 1 to 5) after extraction, followed by incubation for 12 h at 70 °C. The Fe element was then identified using atomic absorption spectrophotometry on each digested sample (0.2 g), which had been diluted with deionized water (50 mL). Fe concentration was reported in mg/100 g of sample. The tissue samples from the brain, liver, spleen, kidney, and tumor were homogenized in saline solution. The amount of EPI in various samples was determined using an HPLC system (Shimadzu, Japan) with a 250 × 4.6 mm column and a mobile phase 0.01 M KH₂PO₄ with a flow rate of 1 mL/min.

2.11. Statistical analysis

Data analysis was performed by SPSS software and data were expressed as mean ± SD of three samples. Statistical comparisons were performed using one-way or two-way analyses of variance (ANOVA). Also, multiple comparisons between treated groups were performed using the Tukey test at the 0.05 level.

3. Results

3.1. Morphological and structural properties

Core-shell IO@Au nanozymes characterized by different techniques and reported in the webpage of the Nanoshel Co. Briefly, it was reported that the prepared core-shell IO@Au nanozymes have a maximum core diameter of 100 nm and shell thickness of 30 nm with a spherical shape.

3.2. Drug loading and release

The EE% of EPI onto the IO@Au nanozymes was determined at 1 h was 84 %. The DL% of EPI to IO@Au nanozymes was 14 %. Also, *in vitro* EPI release assay was performed at pH 7.4 (normal blood) and 6.5 (cancer cells). 81 % free EPI was detected to be rapidly released in the first 12 h, while about 9 % and 41 % EPI was released in physiologic and in acidic conditions, respectively. These findings indicated that the release rate of EPI in a tumor microenvironment would be much higher than in normal tissues.

3.3. Catalytic activity of core-shell nanozymes

As can be seen in Fig. 1A, nanozymes in the presence of H₂O₂ show POD-mimic activity. However, the results show that loading of EPI significantly reduces the catalytic activity of core-shell nanozymes in TMB degradation. Meanwhile, in the presence of EPI, the PDT increases the rate of H₂O₂ decomposition. This means that PDT can mitigate the negative effect of EPI on the catalytic behavior of nanozymes. As a result, the catalytic properties of the core-shell nanozymes for cancer therapeutics are expected to increase with EPI release following application of PDT in tumor tissue.

In the following, the results of O₂ production in Fig. 1B also confirm the CAT-mimic activity of nanozymes. The results show that PDT can increase O₂ production despite the EPI's negative effect on O₂ production by reducing the nanozymes' access to H₂O₂ for CAT-like activity. As a result, it is anticipated that the application of core-shell might effectively overcome the level of hypoxia in tumors over time. Overall, the above findings confirmed that core-shell nanozymes exhibit photo-enhanced catalytic activity.

3.4. Cytotoxicity assay

First, the cytotoxicity of EPI (10 µg/ml) on 4T1 cells was studied and the outcome is presented in Fig. 2. EPI could inhibit the proliferation of

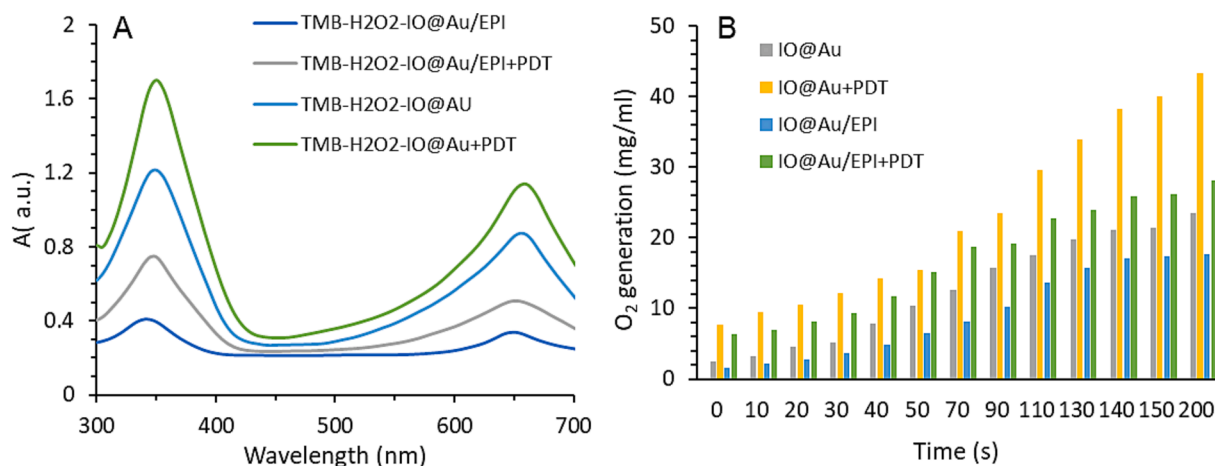


Fig. 1. (A) Peroxidase (POD)-like activity of core-shell nanozymes free or loaded with EPI in the absence and presence of photodynamic therapy (PDT), (B) Catalase (CAT)-like activity of core-shell nanozymes free or loaded with EPI in the absence and presence of photodynamic therapy (PDT).

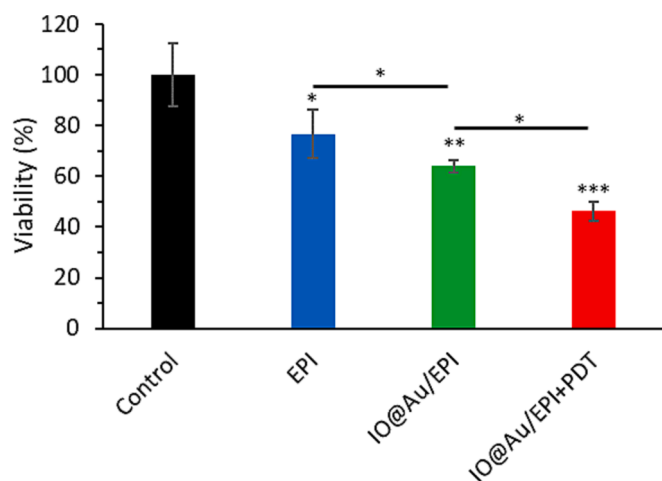


Fig. 2. MTT assay of 4T1 cells treated with free EPI (10 μg/ml) as well as IO@Au nanozymes loaded with EPI (equivalent concentration to 10 μg/ml EPI) for 24 h without and with irradiation (30 mW/cm² laser for 5 min, after 8 h). *P < 0.05, **P < 0.01 and ***P < 0.001.

4T1 cancer cells within 24 h. We then evaluated the effect of IO@Au/EPI on the growth of 4 the 4T1 cells and found that nanoformulation of EPI results in higher cytotoxicity than the free drug. We then investigated

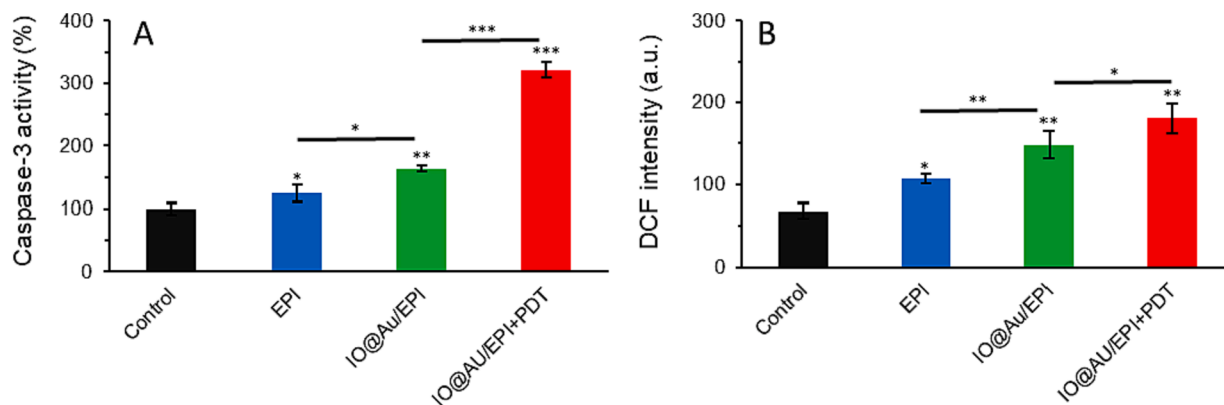


Fig. 3. The cells were treated with free EPI (10 μg/ml) as well as IO@Au nanozymes loaded with EPI (equivalent concentration to 10 μg/ml EPI) for 24 h without and with irradiation (30 mW/cm² laser for 5 min, after 8 h). (A) Caspase-3 activity in 4T1 cancer cells after receiving various treatments, (B) The effect of drug and nanoparticles along with photodynamic therapy (PDT) on ROS production.

the probable potential anticancer effects of IO@Au/EPI in combination with PDT. The data showed an obvious increase in the anti-proliferation effects on used nanozyme (Fig. 2).

3.5. Apoptosis and ROS assay

Fig. 3A confirmed that EPI loading onto the core-shell nanozymes significantly increases cytotoxicity in 4T1 cancer cells by increasing caspase-3 activity compared to the free EPI. In addition, the apoptosis output in Fig. 3A shows that the application of PDT enabled by core-shell nanozymes loaded with EPI further enhanced the apoptotic effects of nanozymes with an additional increase in the activity of caspase-3 in comparison with other treated groups.

The intracellular ROS findings in Fig. 3B confirmed that the combination of chemotherapy and PDT enabled by core-shell nanozymes loaded with EPI resulted in the highest level of ROS generation among other treated groups. Compared to the control, the highest levels of ROS production were linked with core-shell nanozymes loaded with EPI combined with PDT, followed by core-shell nanozymes loaded with EPI and free EPI.

3.6. Tumor and organ condition

The results of Fig. 4A showed that the control group lost weight significantly. Furthermore, the results revealed that when the free EPI was used, the weight of the mice was significantly maintained when

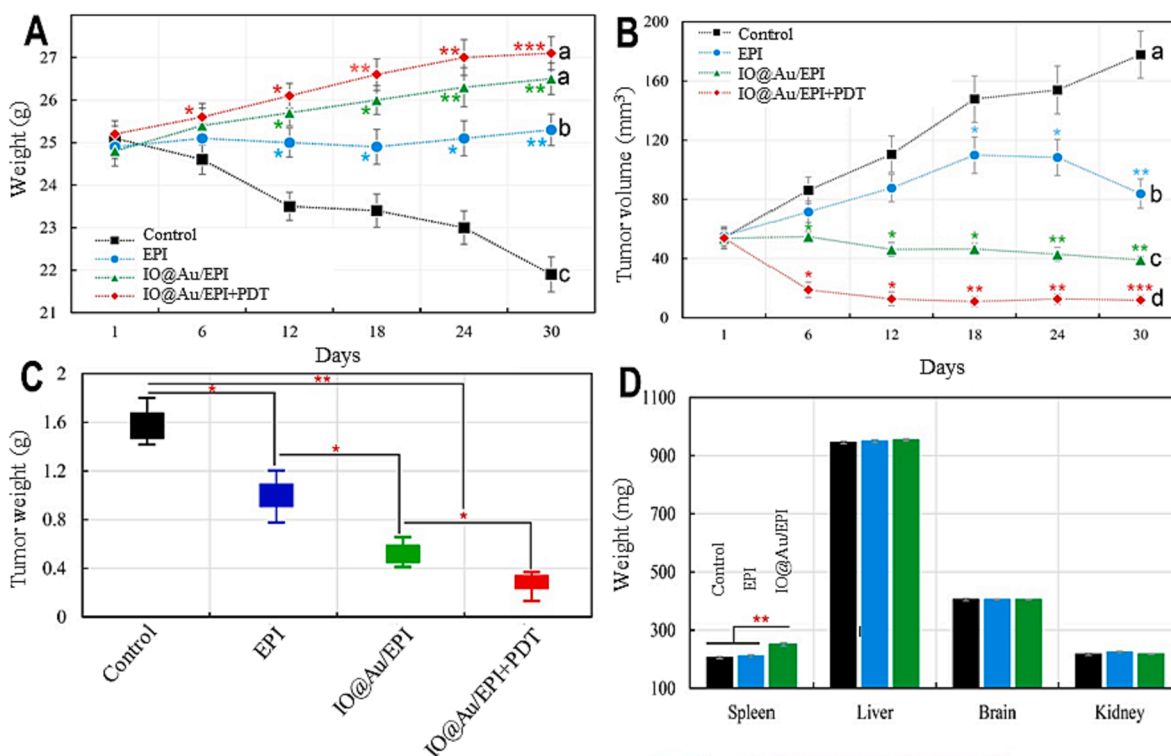


Fig. 4. (A) Time-dependent curve of mice body weight during experiment after injection with EPI (Epirubicin), core-shell nanozymes loaded with EPI, and core-shell nanozymes loaded with EPI in the presence of PDT treatments, (B) Tumor volume change curves of mice after different treatments, (C) The final weight of tumors after different treatments at the end of the experimental period, (D) Weight of main organs of spleen, liver, kidney and brain after treatment of mice with EPI and core-shell nanozymes loaded with EPI. ^{a,b,c,d}Least square means with different letters in superscripts are different at **P* < 0.05. **P* < 0.05, ***P* < 0.01 and ****P* < 0.001.

compared to the control. Overall, the core-shell nanozymes with or without PDT demonstrated the best performance in mice weight. The results of Fig. 4B show that, while the mice treated with core-shell nanozymes loaded with the drug alone or combined with PDT have the lowest tumor volume changes among the treated groups, the mice treated with core-shell nanozymes loaded with the drug combined with PDT have the lowest observed tumor volume. In addition, compared to the control, the utilization of EPI separately reduced tumor volume. In confirmation of the above findings, the results of Fig. 4C show that the combination of core-shell nanozymes loaded with the drug and PDT causes a significant reduction in tumor weight compared to other treated groups at the end of the experimental period. Furthermore, the results of

Fig. 4D show that following the application of core-shell nanozymes loaded with EPI, no significant effect on the weights of the brain, liver, and kidneys was observed when compared to the control and the EPI-treated groups. However, when compared to the control and free EPI-treated groups, the use of core-shell nanozymes loaded with the drug as a drug carrier causes a significant increase in spleen weight.

3.7. Hypoxia and apoptosis mechanisms

The expression level of HIF-1 increases in an oxygen-free environment, which can be used to determine the level of hypoxia in the tumor microenvironment. In this study, the effect of EPI on the expression of

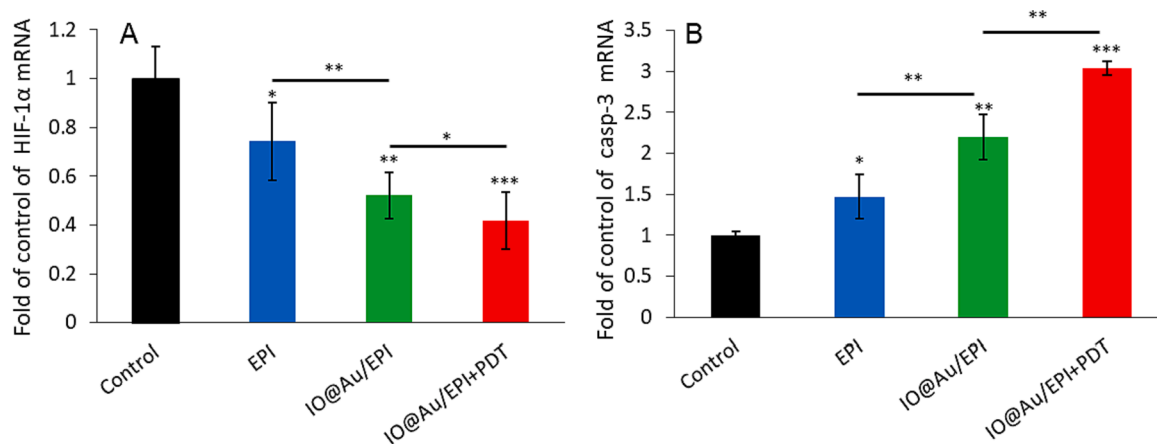


Fig. 5. (A) HIF-1 α gene expression and (B) caspase-3 mRNA expression in the tumor tissue of different samples, including control groups, EPI-treated group, core-shell nanozyme loaded with EPI, and core-shell nanozymes loaded with EPI in the presence of PDT. **P* < 0.05, ***P* < 0.01 and ****P* < 0.001.

HIF-1 α gene in tumor tissues shows that the core-shell nanozymes loaded with EPI reduce significantly the expression of HIF-1 α gene in tumor tissues compared to free EPI and control groups, respectively (Fig. 5A). While the combination of the core-shell nanozymes loaded with EPI in the presence of PDT further reduced the expression of HIF-1 α gene compared to the core-shell nanozymes loaded with EPI. These results, confirm that HIF-1 α gene expression, which increases under hypoxic conditions, decreases significantly in the presence of core-shell nanozymes loaded with EPI with or without PDT (Fig. 5A).

The apoptosis mechanism assay in tumor tissues showed that EPI significantly increased the expression of caspase-3 gene (Fig. 5B) in tumor tissues compared to the control. While the outputs of Fig. 5B showed a significant increase in the expression of caspase-3 gene following the utilization of the core-shell nanozymes loaded with EPI compared to the control. In addition, the combination of chemotherapy and PDT caused significant changes in the expression of caspase-3 gene compared to the free EPI. Taken together, the mitigation of HIF-1 gene expression and upregulation of caspase-3 gene expression enabled by core-shell nanozymes loaded with EPI with or without PDT could be very effective and promising in therapeutic perspectives.

3.8. Fe and drug distribution

Examination of Fe accumulation and bio-distribution shows that 12 h after the final injection of core-shell nanozymes loaded with EPI, the rate of Fe permeability and its retention in tumor tissue increases significantly compared to the control (Fig. 6A). Although the application of core-shell nanozymes loaded with the drug caused a significant increase in Fe concentration in the spleen, they had no effect on Fe concentration in liver, brain, and kidney. Surprisingly, the lack of significant Fe accumulation in the kidney may indicate a decrease in the clearance of core-shell nanozymes loaded with EPI. Overall, the reduction in Fe accumulation in main tissues enabled by core-shell

nanozymes loaded with the drug may indicate a reduction in the EPI's negative effects in off-target tissues. In support of this finding, bio-distribution of the EPI in major tissues revealed that the EPI is significantly targeted in tumor site (Fig. 6B). As shown in Fig. 6B, 12 h after the final injection of core-shell nanozymes loaded with the drug, EPI accumulation in tumor tissues increased significantly compared to free EPI, while the concentration of EPI was significantly lower in the brain, liver, and kidney compared to free EPI. Among these, the lowest concentration of EPI was related to the brain, which can cause low toxicity in the treatment process, similar to the lack of Fe concentration.

4. Discussion

Although EPI is thought to be a promising anticancer agent, its severe side effects against off-target tissues and the requirement for high drug concentrations in anticancer activities limit its potential for use in a wide range of applications. Recent studies have demonstrated an improvement in anticancer drug accumulation in the tumor site using different nanomaterials functionalized with various targeting moieties or synthesized with pH-sensitive materials (Luiz et al., 2021). Smart materials-based nanomaterial platforms can show rapid phase transitions upon reaching the tumor microenvironment, thereby resulting in a release in their cargoes at the tumor site. Core-shell nanostructures have been shown to serve as a great candidates in drug delivery as well as a combination treatment of cancer cells (Habib et al., 2008, Menon et al., 2017, Zhang et al., 2023). In the present study, we used core-shell nanozymes and used them in improved combined chemo-PDT of breast cancer.

The study's findings, which concur with those of Gao et al. (2017b), Alijani et al., 2020 and Laha et al., 2019 confirmed that the more promising inhibitory effect of the core-shell nanozymes loaded with the drug on inhibiting the growth of 4T1 cancer cells compared to free EPI is primarily due to increased intracellular ROS generation and associated apoptosis.

The *in vivo* results in this study, consistent with the findings of Laha et al., 2019 show that the core-shell nanozymes loaded with EPI have significant efficacy in improving mice weight and reducing the weight of tumors when compared to free EPI. Also consistent with previous findings (Wang et al., 2018, Hou et al., 2019), it was discovered that combining chemotherapy and PDT with increasing intracellular ROS generation via the developed platform's POD-like activity has a significant effect on tumor weight loss. However, Xiang et al. (2020) showed that the core-shell nanozymes do not provide us with a significant difference in the weight of mice compared to the free drug. In addition, in line with the results of Xiang et al. (2020) and Liu et al. (2020), the anti-tumor efficacy of core-shell nanozymes loaded with the drug is attributed to increased Fe retention and high EPI accumulation in tumor tissue. Therefore according to the findings of Yen et al. (2019), the application of core-shell nanozymes might overcome tumor tissue hypoxia by producing O₂ via possible H₂O₂ degradation in tumor tissue. In fact, it has previously been demonstrated that increasing drug permeability to solid tumors reduces tumor size and is directly related to increased O₂ level (Ikeda et al., 2016, Nie et al., 2022, Sharifi et al., 2022). However, consistent with the finding of Cheng et al. (2020) we showed that the combination of chemotherapy and PDT enabled by core-shell nanozymes might overcome hypoxia toward the enhancement of tumor therapy. In this regard, Ma et al., 2019 and Yang et al., 2020 found that the utilization of drugs with hypoxia-overcoming nanoparticles can enhance the production of ROS in tissue and increase drug permeability.

Finally, this study demonstrates that the use of core-shell nanozymes for tumor treatment is a potential strategy due to high drug loading, controlled pH-sensitive drug release, chemo-photodynamic combination cancer therapy, and increasing drug toxicity in 4T1 cancer cells.

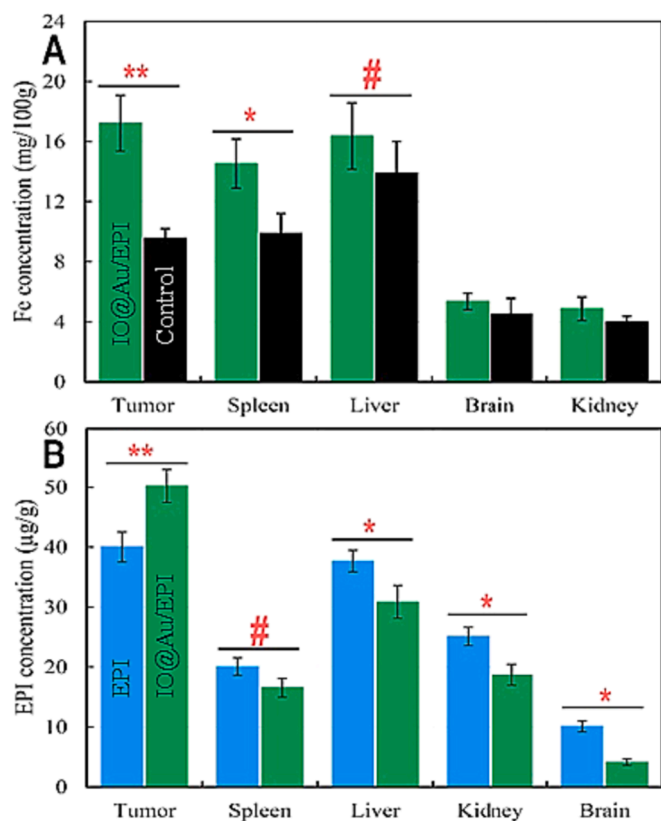


Fig. 6. The distribution of iron (Fe) (A) and Epirubicin (EPI) (B) in the kidney, brain, liver, spleen, and tumor tissues. #P < 0.10, *P < 0.05, **P < 0.01.

5. Conclusions

In general, it was shown that used core-shell nanozymes have photo-enhanced catalytic activity. Also, core-shell nanozymes loaded with the drug showed apoptosis induction mediated by high levels of intracellular ROS. Furthermore, the reduction of EPI accumulation in off-target tissues are the potential advantage of the core-shell nanozymes, which ultimately resulted in a significant reduction of tumor size through decrease of HIF-1 α gene expression and overexpression of caspase-3 gene to overcome tumor hypoxia and induce apoptosis, respectively. Further, *in vivo* observations illuminate that the core-shell nanozymes have high potential in chemo-photodynamic combination therapy for improving breast cancer treatment. Although these findings support the application of core-shell nanozymes as promising nanoparticle-based drug delivery systems for cancer therapy, further studies are needed in future investigations.

Additional information

No additional information is available for this paper.

Ethics approval and consent to participate

All animal use procedures were carried out in accordance with the Regulations of Animal Care and Use Committee of the Department of Radiation Oncology, Affiliated Cancer Hospital of Inner Mongolia Medical University with the approval of the Ethics Committee.

Declaration of competing interest

The authors declare that they have no known competing financial interests or personal relationships that could have appeared to influence the work reported in this paper.

References

- Alijani, H., Noori, A., Faridi, N., Bathaie, S.Z., Mousavi, M.F., 2020. Aptamer-functionalized Fe₃O₄@ MOF nanocarrier for targeted drug delivery and fluorescence imaging of the triple-negative MDA-MB-231 breast cancer cells. *J. Solid State Chem.* 292, 121680.
- Alizadeh, N., Salimi, A., Sham, T.-K., Bazylewski, P., Fanchini, G., Fathi, F., Soleimani, F., 2021. Hierarchical Co (OH) 2/FeOOH/WO3 ternary nanoflowers as a dual-function enzyme with pH-switchable peroxidase and catalase mimic activities for cancer cell detection and enhanced photodynamic therapy. *Chem. Eng. J.* 417, 129134.
- Chatterjee, K., Sarkar, S., Rao, K.J., Paria, S., 2014. Core/shell nanoparticles in biomedical applications. *Adv. Colloid Interface Sci.* 209, 8–39.
- Cheng, X., He, L., Xu, J., Fang, Q., Yang, L., Xue, Y., Wang, X., Tang, R., 2020. Oxygen-producing catalase-based prodrug nanoparticles overcoming resistance in hypoxia-mediated chemo-photodynamic therapy. *Acta Biomaterialia* 112, 234–249.
- Danafar, H., Sharafi, A., Manjili, H.K., 2018. Co-delivery of sulfuraphane and curcumin with PEGylated iron oxide-gold core shell nanoparticles for delivery to breast cancer cell line. *Iran. J. Pharmaceut. Res.: LJPR* 17 (2), 480.
- Feng, N., Li, Q., Bai, Q., Xu, S., Shi, J., Liu, B., Guo, J., 2022. Development of an Au-anchored Fe Single-atom nanozyme for biocatalysis and enhanced tumor photothermal therapy. *J. Colloid Interface Sci.* 618, 68–77.
- Gao, L., Fan, K., Yan, X., 2017a. Iron oxide nanozyme: a multifunctional enzyme mimetic for biomedical applications. *Theranostics* 7 (13), 3207.
- Gao, X., Zhai, M., Guan, W., Liu, J., Liu, Z., Damirin, A., 2017b. Controllable synthesis of a smart multifunctional nanoscale metal-organic framework for magnetic resonance/optical imaging and targeted drug delivery. *ACS Appl. Mater. Interfaces* 9 (4), 3455–3462.
- Gurunathan, S., Kang, M.-H., Qasim, M., Kim, J.-H., 2018. Nanoparticle-mediated combination therapy: Two-in-one approach for cancer. *Int. J. Mol. Sci.* 19 (10), 3264.
- Habib, A., Ondeck, C., Chaudhary, P., Bockstaller, M., McHenry, M., 2008. Evaluation of iron-cobalt/ferrite core-shell nanoparticles for cancer chemotherapy. *J. Appl. Phys.* 103 (7), 07A307.
- Hou, H., Huang, X., Wei, G., Xu, F., Wang, Y., Zhou, S., 2019. Fenton reaction-assisted photodynamic therapy for cancer with multifunctional magnetic nanoparticles. *ACS Appl. Mater. Interfaces* 11 (33), 29579–29592.
- Ikedo, Y., Hisano, H., Nishikawa, Y., Nagasaki, Y., 2016. Targeting and treatment of tumor hypoxia by newly designed prodrug possessing high permeability in solid tumors. *Mol. Pharm.* 13 (7), 2283–2289.
- Irvin Jr, W.J., Carey, L.A., 2008. What is triple-negative breast cancer? *Eur. J. Can.* 44 (18), 2799–2805.
- Khan, S., Falahati, M., Cho, W.C., Vahdani, Y., Siddique, R., Sharifi, M., Jaragh-Alhadad, L.A., Haghghat, S., Zhang, X., Ten Hagen, T.L., 2023. Core-shell inorganic NPs@ MOF nanostructures for targeted drug delivery and multimodal imaging-guided combination tumor treatment. In: *Advances in Colloid and Interface Science*, p. 103007.
- Laha, D., Pal, K., Chowdhuri, A.R., Parida, P.K., Sahu, S.K., Jana, K., Karmakar, P., 2019. Fabrication of curcumin-loaded folic acid-tagged metal organic framework for triple negative breast cancer therapy in vitro and in vivo systems. *New J. Chem.* 43 (1), 217–229.
- Lane, D., 2006. Designer combination therapy for cancer. *Nat. Biotechnol.* 24 (2), 163–164.
- Lee, H., Han, J., Shin, H., Han, H., Na, K., Kim, H., 2018. Combination of chemotherapy and photodynamic therapy for cancer treatment with sonoporation effects. *J. Control. Release* 283, 190–199.
- Li, W., Peng, J., Tan, L., Wu, J., Shi, K., Qu, Y., Wei, X., Qian, Z., 2016. Mild photothermal therapy/photodynamic therapy/chemotherapy of breast cancer by Lyp-1 modified Docetaxel/IR820 Co-loaded micelles. *Biomaterials* 106, 119–133.
- Li, J., Zhou, Y., Yan, S., Wu, W., Sharifi, M., 2023. Core-shell iron oxide-platinum@ metal organic framework/epirubicin nanospheres: synthesis, characterization and anti-breast cancer activity. *Arab. J. Chem.* 16 (11), 105229.
- Liu, P., Liu, X., Cheng, Y., Zhong, S., Shi, X., Wang, S., Liu, M., Ding, J., Zhou, W., 2020. Core-shell nanosystems for self-activated drug-gene combinations against triple-negative breast cancer. *ACS Appl. Mater. Interfaces* 12 (48), 53654–53664.
- Lu, Y., Ye, W., Yang, Q., Yu, J., Wang, Q., Zhou, P., Wang, C., Xue, D., Zhao, S., 2016. Three-dimensional hierarchical porous PtCu dendrites: a highly efficient peroxidase nanozyme for colorimetric detection of H₂O₂. *Sens. Actuat. B* 230, 721–730.
- Luiz, M.T., Dutra, J.A.P., Di Filippo, L.D., Junior, A.G.T., Tofani, L.B., Marchetti, J.M., Chorilli, M., 2021. Epirubicin: biological properties, analytical methods, and drug delivery nanosystems. *Crit. Rev. Anal. Chem.* 1–14.
- Ma, Z., Wu, L., Han, K., Han, H., 2019. Pt nanozyme for O₂ self-sufficient, tumor-specific oxidative damage and drug resistance reversal. *Nanoscale Horiz.* 4 (5), 1124–1131.
- Menon, J.U., Kuriakose, A., Iyer, R., Hernandez, E., Gandee, L., Zhang, S., Takahashi, M., Zhang, Z., Saha, D., Nguyen, K.T., 2017. Dual-drug containing core-shell nanoparticles for lung cancer therapy. *Sci. Rep.* 7 (1), 1–13.
- Mokhtari, R.B., Homayouni, T.S., Baluch, N., Morgatskaya, E., Kumar, S., Das, B., Yeger, H., 2017. Combination therapy in combating cancer. *Oncotarget* 8 (23), 38022.
- Nie, Z., Vahdani, Y., Cho, W.C., Bloukh, S.H., Edis, Z., Haghghat, S., Falahati, M., Kheradmandi, R., Jaragh-Alhadad, L.A., Sharifi, M., 2022. 5-Fluorouracil-containing inorganic iron oxide/platinum nanozymes with bimodal drug delivery and peroxidase-like activity for the treatment of breast cancer. *Arab. J. Chem.* 103966.
- Sharifi, M., Hasan, A., Nanakali, N.M.Q., Salih, A., Qadir, F.A., Muhammad, H.A., Shekha, M.S., Aziz, F.M., Amen, K.M., Najafi, F., 2020. Combined chemo-magnetic field-photothermal breast cancer therapy based on porous magnetite nanospheres. *Sci. Rep.* 10 (1), 5925.
- Sharifi, M., Cho, W.C., Ansariesfahani, A., Tarharoudi, R., Malekisarvar, H., Sari, S., Bloukh, S.H., Edis, Z., Amin, M., Gleghorn, J.P., 2022. An updated review on EPR-based solid tumor targeting nanocarriers for cancer treatment. *Cancers* 14 (12), 2868.
- Sharifi, M., Kheradmandi, R., Alizadeh, M., 2023. Two birds with one stone: triple negative breast cancer therapy by PtCo bimetallic nanozyme coated with gemcitabine-hyaluronic acid-polyethylene glycol. *Cancer Nanotechnol.* 14 (1), 1–20.
- Wang, X., Xu, J., Yang, D., Sun, C., Sun, Q., He, F., Gai, S., Zhong, C., Li, C., Yang, P., 2018. Fe₃O₄@ MIL-100 (Fe)-UCNPs heterojunction photosensitizer: rational design and application in near infrared light mediated hypoxic tumor therapy. *Chem. Eng. J.* 354, 1141–1152.
- Xiang, Z., Qi, Y., Lu, Y., Hu, Z., Wang, X., Jia, W., Hu, J., Ji, J., Lu, W., 2020. MOF-derived novel porous Fe₃O₄@ C nanocomposites as smart nanomedical platforms for combined cancer therapy: magnetic-triggered synergistic hyperthermia and chemotherapy. *J. Mater. Chem. B* 8 (37), 8671–8683.
- Xu, D., Wu, L., Yao, H., Zhao, L., 2022. Catalase-like nanozymes: classification, catalytic mechanisms, and their applications. *Small* 18 (37), 2203400.
- Yang, Y., Zhu, D., Liu, Y., Jiang, B., Jiang, W., Yan, X., Fan, K., 2020. Platinum-carbon-integrated nanozymes for enhanced tumor photodynamic and photothermal therapy. *Nanoscale* 12 (25), 13548–13557.
- Yen, T.Y., Stephen, Z.R., Lin, G., Mu, Q., Jeon, M., Untoro, S., Welsh, P., Zhang, M., 2019. Catalase-functionalized iron oxide nanoparticles reverse hypoxia-induced chemotherapeutic resistance. *Adv. Healthc. Mater.* 8 (20), 1900826.
- Zeng, X., Ruan, Y., Chen, Q., Yan, S., Huang, W., 2023. Biocatalytic cascade in tumor microenvironment with a Fe₂O₃/Au hybrid nanozyme for synergistic treatment of triple negative breast cancer. *Chem. Eng. J.* 452, 138422.
- Zhang, X., Xu, C.-H., Mo, J., Zheng, X.-J., Chen, Y.-F., Yang, A.-Q., Zhang, Y.-H., Wang, P.-Y., Yuan, X., Ye, X.-S., 2023. Self-assembled core-shell nanoscale coordination polymer nanoparticles carrying a sialyltransferase inhibitor for cancer metastasis inhibition. *ACS Appl. Mater. Interfaces* 15 (6), 7713–7724.